A case of well-differentiated hepatocellular carcinoma detected with 18F-PSMA-1007 positron emission tomography-computed tomography

Zhijun Wang[1#], Yingzhen Cong[2#], Yingdan Jiang[1#], Lu Shi[1#]

[1]Department of Nuclear Medicine, Weihai Central Hospital, Qingdao University, Weihai, China; [2]Department of Health Service, Weihai Central Hospital, Qingdao University, Weihai, China

[#]These authors contributed equally to this work.

Correspondence to: Lu Shi, Master. Department of Nuclear Medicine, Weihai Central Hospital, Qingdao University, No. 3, Mishan East Road, Weihai 264000, China. Email: shilu0127@163.com.

Introduction

Hepatocellular carcinoma (HCC) is the most common type of primary liver cancer, accounting for approximately 85–90% of all cases (1). HCC is unique among malignancies on imaging, allowing for an accurate diagnosis without an invasive biopsy. Multiphasic computed tomography (CT) and magnetic resonance imaging (MRI) are both used for the noninvasive diagnosis of HCC in patients with cirrhosis and an indeterminate mass (2). Prostate-specific membrane antigen (PSMA) is a glycosylated type II transmembrane protein, which serves as a biomarker for prostate cancer and is often targeted in diagnostic and therapeutic approaches for this type of cancer. A recent meta-analysis of 6 studies using ^{68}Ga-PSMA-11 reported that PSMA-targeting radiopharmaceuticals were found to provide a detection rate of 85% for positron emission tomography (PET) imaging in the diagnosis of HCC (3). We reported a case of an isolated well-differentiated HCC pathologically proven and ^{18}F-PSMA-1007 avid on PET-CT.

Case presentation

The patient was a 78-year-old man with a history of hepatitis B and liver cirrhosis for many years, and his blood tests showed high values of alpha-fetoprotein (AFP).

Contrast-enhanced MRI showed multiple abnormal signal foci in the liver, and hepatocellular liver cancer was highly suspected (*Figure 1A-1E*). Subsequent fine-needle aspiration (FNA) biopsy showed presence of malignant cells that resembled well-differentiated hepatocytes with numerous stripped atypical nuclei and macronucleoli, which were pathologically confirmed as HCCs (*Figure 1F*). The ^{18}[F]-fluorodeoxyglucose (^{18}F-FDG) PET-CT scan showed multiple round and slightly low-density foci in the liver. The largest lesion was located in the S8 segment with a size of 4.19×4.37 cm, and its edge was not clear. The radioactive uptake of this lesion was similar to that of the surrounding normal liver tissue with a maximum standardized uptake value (SUVmax) of 3.3 (*Figure 2A-2D*). However, ^{18}F-PSMA-1007 PET-CT showed abnormal radioactive uptake at the corresponding site with a SUVmax of 25.6 (*Figure 2E-2H*). The patient subsequently continued to undergo multiple interventional embolization treatments. Unfortunately, the patient died after a year and a half of follow-up.

All procedures conducted in this study adhered to the ethical standards set by the institutional and/or national research committee(s) and with the Helsinki Declaration (as revised in 2013). Written informed consent was obtained from the patient for publication of this case report and accompanying images. A copy of the written consent is available for review by the editorial office of this journal.
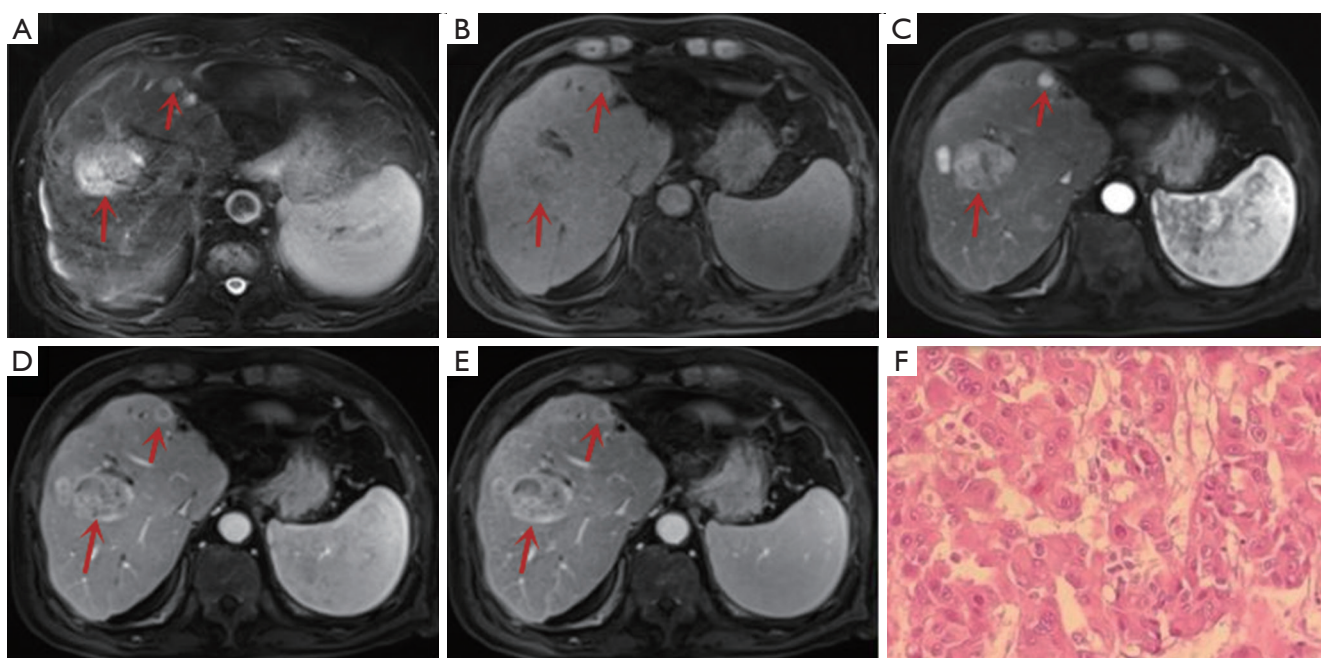
Figure 1 The MRI images and pathology of a 78-year-old male patient with well-differentiated HCC (red arrows). MRI T2WI (A) showed 2 liver lesions with high signal intensity, and MRI T1WI (B) showed hypointensity for the same lesions. Contrast-enhanced MRI (C-E) showed 2 lesions with enhancement in the early stage and washout in the delayed phase, with the lesions being significantly enhanced in the arterial phase. Pathology of the right lobe node (F) indicated highly differentiated HCC (HE, ×200). MRI, magnetic resonance imaging; HCC, hepatocellular carcinoma; T2WI, T2-weighted imaging; T1WI, T1-weighted imaging; HE, hematoxylin and eosin.

Discussion

HCC is the most common form of liver cancer and has a relatively low 5-year survival rate. Chronic hepatitis infections leading to liver cirrhosis attribute to the major risk factors. Multiphasic CT or MRI can be used for the diagnosis of HCC, in which HCC commonly shows enhancement as compared with surrounding parenchyma in the early arterial phase and washout in the delayed phase (4). However, a prospective study indicated that the negative value of traditional noninvasive imaging diagnosis is up to 9% (5). Due to the absences of evidence for early diagnosis, most patients are diagnosed at advanced stage leading to poor prognosis. Thus, developing new imaging tools for the diagnosis and prognosis of HCC is crucial.

Based on glucose metabolism, ^{18}F-FDG PET-CT is a functional imaging modality for diagnosis, staging, restaging, and treatment monitoring with high sensitivity and specificity. However, PET-CT imaging with ^{18}F-FDG has a limited role in HCC due to its low radioactive uptake (6). Research indicates that the detection rate for ^{18}F-FDG in well-differentiated HCC is approximately 44% (7). Other high-sensitive radioactive agents including ^{18}F-fluorocholine and ^{11}C-acetate have a relatively poorer availability because of a short half-life and lower image resolution, leading to limited use in routine clinical practice (8).

PSMA is a transmembrane protein, which is expressed on prostate epithelial cells and overexpressed on the surface of prostatic adenocarcinoma cells. One retrospective study reported that PSMA was expressed in the neovasculature of various types of malignancies other than prostate cancer, regulating tumor cell invasion and tumor angiogenesis (9). In a study by Rizzo *et al.*, the incidental uptake of PSMA was discovered in other nonprostatic solid tumors, including HCC (10). An immunohistochemistry study on HCC reported that PSMA expression was high in tumor tissues, with canalicular and neovascular pattern types (11). In another study, the percentage of PSMA expression in the tumor-associated neovascular endothelium was higher than that in liver cirrhosis (12). Since there is a preferential accumulation of PSMA in tumor tissue compared to normal liver tissue, PET images can clearly display the tumor
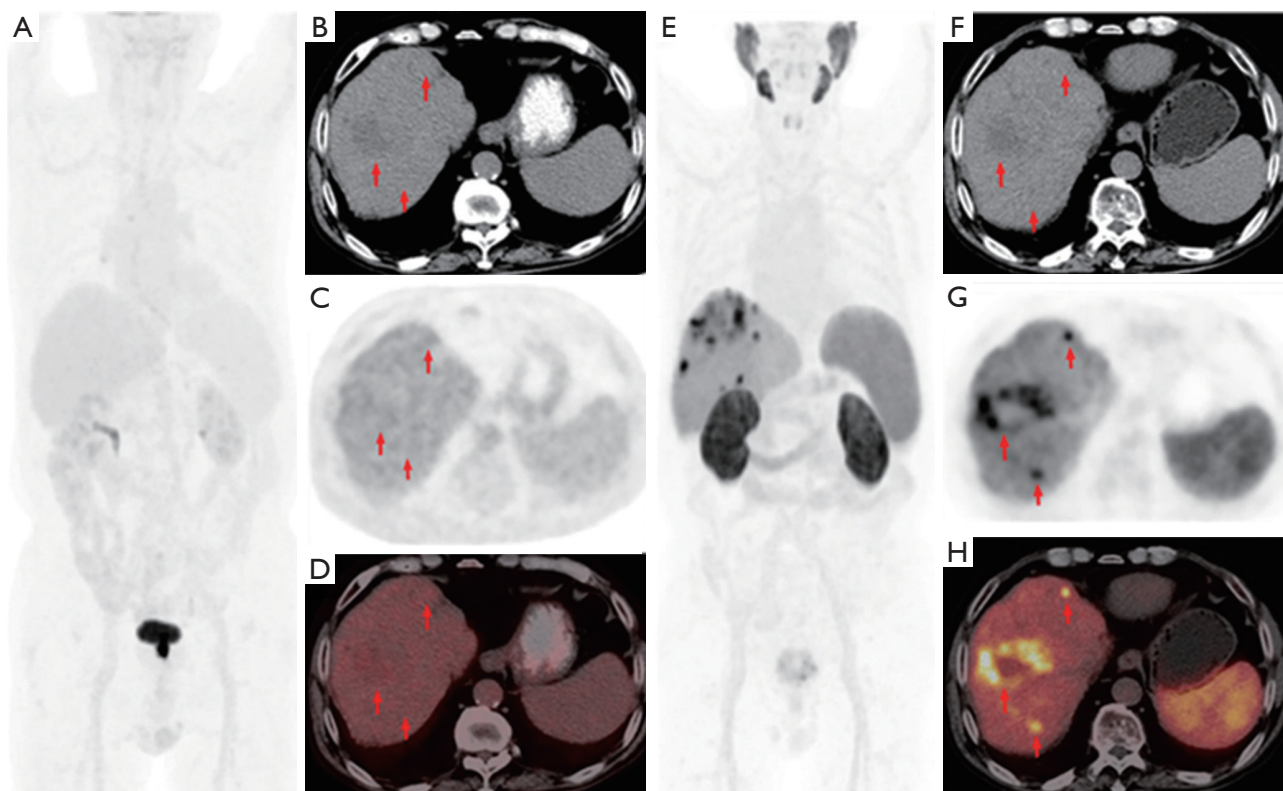
7376

Wang et al. Hepatocellular carcinoma on ^{18}F-PSMA-1007 PET-CT

Figure 2 The MIP of ^{18}F-FDG PET-CT (A) and ^{18}F-PSMA-1007 PET-CT (E). The plain CT image (B), PET image (C), and ^{18}F-FDG PET-CT fusion image (D) showed multiple round and slightly low-density foci in the liver (red arrows). The SUVmax of the largest lesion located in the S8 segment with a size of 4.19×4.37 cm was 3.3, similar to that of the surrounding normal liver tissue. The plain CT image (F), PET image (G), and ^{18}F-PSMA-1007 PET-CT fusion image (H) showed abnormal radioactive uptake at the corresponding site with a SUVmax of 25.6 (red arrows). MIP, maximum intensity projection; ^{18}F-FDG, ^{18}[F]-fluorodeoxyglucose; PET-CT, positron emission tomography-computed tomography; PSMA, prostate-specific membrane antigen; SUVmax, maximum standardized uptake value.

locations. It is thus possible to use PSMA PET imaging in the detection of primary HCC lesions (13). Hirmas *et al.* reported that ^{68}Ga-PSMA-11 PET demonstrated higher accuracy than did CT in the detection of HCC metastases and was associated with a management change in about half of the patient cohort (14). Our semiquantitative analysis revealed a SUVmax of 25.6 for HCC with ^{18}F-PSMA-1007, and it was higher than that described by Gündoğan *et al.* with ^{68}Ga-PSMA (15). ^{68}Ga-PSMA PET-CT has demonstrated a marked superiority to ^{18}F-FDG PET-CT in terms of HCC staging (15). The endpoint positron energy of ^{18}F-labeled PSMA ligands is much lower than that of ^{68}Ga (0.65 *vs.* 1.90 MeV), which reduces the positron range in tissue and may improve spatial resolution (16). In clinic, the different physical properties of the nuclides may influence the quantitative uptakes of ^{18}F-PSMA and ^{68}Ga-PSMA, but few clinical studies have directly compared ^{18}F-PSMA and

^{68}Ga-PSMA in the liver region. This is the first report of well-differentiated HCC being detected on ^{18}F-PSMA-1007 PET-CT, with false-negative ^{18}F-FDG PET findings showing low ^{18}F-FDG accumulation in PET images. More prospective studies are required to investigate the disparity in the initial characterization between ^{18}F-PSMA and ^{68}Ga-PSMA for indeterminate liver lesions and their relevance in staging, particularly prior to surgical interventions.

Conclusions

Our report supports the potential application of ^{18}F-PSMA-1007 PET-CT in well-differentiated HCC, encouraging further studies in a larger patient cohort. Prospective investigations into the utility of PSMA imaging or therapy could provide valuable insights and potential benefits for patients diagnosed with HCC.

References

1. Forner A, Reig M, Bruix J. Hepatocellular carcinoma. Lancet 2018;391:1301-14.
2. Roberts LR, Sirlin CB, Zaiem F, Almasri J, Prokop LJ, Heimbach JK, Murad MH, Mohammed K. Imaging for the diagnosis of hepatocellular carcinoma: A systematic review and meta-analysis. Hepatology 2018;67:401-21.
3. Rizzo A, Racca M, Albano D, Dondi F, Bertagna F, Annunziata S, Treglia G. Can PSMA-Targeting Radiopharmaceuticals Be Useful for Detecting Hepatocellular Carcinoma Using Positron Emission Tomography? An Updated Systematic Review and Meta-Analysis. Pharmaceuticals (Basel) 2022;15:1368.
4. Vogel A, Meyer T, Sapisochin G, Salem R, Saborowski A. Hepatocellular carcinoma. Lancet 2022;400:1345-62.
5. Childs A, Zakeri N, Ma YT, O'Rourke J, Ross P, Hashem E, Hubner RA, Hockenhull K, Iwuji C, Khan S, Palmer DH, Connor J, Swinson D, Darby S, Braconi C, Roques T, Yu D, Luong TV, Meyer T. Biopsy for advanced hepatocellular carcinoma: results of a multicentre UK audit. Br J Cancer 2021;125:1350-5.
6. Izuishi K, Yamamoto Y, Mori H, Kameyama R, Fujihara S, Masaki T, Suzuki Y. Molecular mechanisms of [18F] fluorodeoxyglucose accumulation in liver cancer. Oncol Rep 2014;31:701-6.
7. Ghidaglia J, Golse N, Pascale A, Sebagh M, Besson FL. 18F-FDG /18F-Choline Dual-Tracer PET Behavior and Tumor Differentiation in HepatoCellular Carcinoma. A Systematic Review. Front Med (Lausanne) 2022;9:924824.
8. Haug AR. Imaging of primary liver tumors with positron-emission tomography. Q J Nucl Med Mol Imaging 2017;61:292-300.
9. Uijen MJM, Derks YHW, Merkx RIJ, Schilham MGM, Roosen J, Privé BM, van Lith SAM, van Herpen CML, Gotthardt M, Heskamp S, van Gemert WAM, Nagarajah J. PSMA radioligand therapy for solid tumors other than prostate cancer: background, opportunities, challenges, and first clinical reports. Eur J Nucl Med Mol Imaging 2021;48:4350-68.
10. Rizzo A, Dall'Armellina S, Pizzuto DA, Perotti G, Zagaria L, Lanni V, Treglia G, Racca M, Annunziata S. PSMA Radioligand Uptake as a Biomarker of Neoangiogenesis in Solid Tumours: Diagnostic or Theragnostic Factor? Cancers (Basel) 2022;14:4039.
11. Tolkach Y, Goltz D, Kremer A, Ahmadzadehfar H, Bergheim D, Essler M, Lam M, de Keizer B, Fischer HP, Kristiansen G. Prostate-specific membrane antigen expression in hepatocellular carcinoma: potential use for prognosis and diagnostic imaging. Oncotarget 2019;10:4149-60.
12. Chen LX, Zou SJ, Li D, Zhou JY, Cheng ZT, Zhao J, Zhu YL, Kuang D, Zhu XH. Prostate-specific membrane antigen expression in hepatocellular carcinoma, cholangiocarcinoma, and liver cirrhosis. World J Gastroenterol 2020;26:7664-78.
13. Lu Q, Long Y, Fan K, Shen Z, Gai Y, Liu Q, Jiang D, Cai W, Wan C, Lan X. PET imaging of hepatocellular carcinoma by targeting tumor-associated endothelium using [68Ga]Ga-PSMA-617. Eur J Nucl Med Mol Imaging 2022;49:4000-13.
14. Hirmas N, Leyh C, Sraieb M, Barbato F, Schaarschmidt

BM, Umutlu L, Nader M, Wedemeyer H, Ferdinandus J, Rischpler C, Herrmann K, Costa PF, Lange CM, Weber M, Fendler WP. (68)Ga-PSMA-11 PET/CT Improves Tumor Detection and Impacts Management in Patients with Hepatocellular Carcinoma. J Nucl Med 2021;62:1235-41.

15. Gündoğan C, Ergül N, Çakır MS, Kılıçkesmez Ö, Gürsu RU, Aksoy T, Çermik TF. (68)Ga-PSMA PET/CT Versus (18)F-FDG PET/CT for Imaging of Hepatocellular Carcinoma. Mol Imaging Radionucl Ther 2021;30:79-85.

16. Hoberück S, Löck S, Borkowetz A, Sommer U, Winzer R, Zöphel K, Fedders D, Michler E, Kotzerke J, Kopka K, Hölscher T, Braune A. Intraindividual comparison of [68 Ga]-Ga-PSMA-11 and [18F]-F-PSMA-1007 in prostate cancer patients: a retrospective single-center analysis. EJNMMI Res 2021;11:109.